Arabian Journal of Geosciences (2021) 14: 1362
https://doi.org/10.1007/s12517-021-07669-0

ORIGINAL PAPER

Spatial modelling for identification of groundwater potential zones in semi-arid ecosystem of southern India using Sentinel-2 data, GIS and bivariate statistical models

Karikkathil C. Arun Kumar[1,2] · Gangalakunta P. Obi Reddy[1] · Palanisamy Masilamani[2] · Pundoor Sandeep[1,2]

Received: 14 September 2020 / Accepted: 3 May 2021 / Published online: 12 July 2021
© Saudi Society for Geosciences 2021

Abstract

The overarching goal of the present investigation is to adopt GIS-based spatial modelling techniques to delineate the groundwater potential zones (GWPZs) in Sarabanga watershed (SBW) of Salem district, Tamil Nadu (TN) state of southern India, by using high-resolution Sentinel-2 data, geographic information system (GIS), and bivariate statistical models (BSM) of frequency ratio (FR), and index of entropy (IoE). In GIS-based spatial modelling, eight contributing factors to groundwater potential (GWP), which includes geology, geomorphology, drainage density (Dd), slope, lineament density (Ld), soil texture, rainfall, land use/land cover (LU/LC), and the well inventory data of 135 well locations were considered in identification of GWPZs. The identified GWPZs of SBW based on the FR, and IoE models show that about 67.8% and 66.1% area of SBW are under very good to excellent categories, while 9.0% and 8.1% are under poor, and very poor categories. The results obtained were validated by using 'Area Under the Curve-Receiver Operating Characteristic' (AUC-ROC) method with the validation data and observed the prediction rate of 0.7313 and 0.7084, for FR, and IoE models, respectively. Modelling of GWPZs shows that FR model clearly exhibits its robustness over the IoE model. Sensitivity analysis performed through Variable Importance Analysis (VIA) indicates that in both FR, and IoE models, geology, slope, rainfall, and Dd were identified as the most influencing factors in delineation of GWPZs. The study clearly demonstrates the potential of Sentinal-2A data, GIS-based spatial modelling, and robustness of FR, and IoE models in attaining the reliable, and cost-effective results in delineation of GWPZs, which helps immensely in development of GW exploration, and management plans.

Keywords Sentinel-2 data · Groundwater · Spatial modelling · Semi-arid ecosystem · Bivariate statistical models

Introduction

Groundwater (GW) is vital for life on earth, and its demand has increased tremendously due to increasing of population, agricultural, industrial, and domestic usages (FAO 2011; Wang et al. 2020; Su et al. 2020). Globally, it was reported that about 42%, 36%, and 27% of net GW withdrawal were consumed by agriculture, domestic, and industrial uses, respectively (Taylor et al. 2013; Ren et al. 2021). Owing to the changes projected in global climate and ever-increasing demand for GW, the urgent adoption of quantitative approaches is essential to assess GW availability and its demand (Chen et al. 2015). In India, nearly 90% of rural and 30% of urban population depend on GW in meeting their basic needs (Agarwal and Garg 2016). Further, the over utilization of GW sources is prevalent in the absence of adequate scientific plans and regulatory mechanisms (Rodell et al. 2009). In recent years, many states of India have experienced the rapid decline of GW level due to increased overexploitation (CWC and CGWB 2016). Many researchers conducted the studies on dynamics of GW and its impacts on agriculture in the changing climate scenarios (Song and Choi 2012) and its overall sustainability (Woo 2013). In order to formulate GW management policies, and priorities, the reliable datasets on groundwater potential (GWP) and its productivity

Responsible Editor: Broder J. Merkel

✉ Gangalakunta P. Obi Reddy
obireddygp@gmail.com

[1] Division of Remote Sensing Applications, ICAR-National Bureau of Soil Survey and Land Use Planning, Amravati Road, Nagpur 440033, India

[2] Department of Geography, Bharathidasan University, Tiruchirappalli, Tamil Nadu 620024, India

are important for policymakers (Das 2017; Etikala et al. 2019). Geological characteristics of the region, it includes type, and porosity of rock formations that primarily determine the GW availability and occurrence (Reddy et al. 1994). The underlying lithological formations control the percolation, and the extent of GW recharge (Shaban et al. 2006). Many authors employed the traditional methods based geological, hydrogeological, and geophysical techniques in delineation of groundwater potential zones (GWPZs) (Chatterji et al. 1978; Rashid et al. 2011; Kumar et al. 2014). The conventional approaches followed in delineation of GWPZs are complex, uneconomical, time-consuming, and have one or other limitations (Jha et al. 2010).

Therefore, precisely identification of GWPZs and device appropriate management strategies by using advance tools, and techniques like remote sensing, Geographic Information System (GIS), and statistical models are important for sustainable development especially in agrarian countries like India. Globally, various techniques such as integration of remote sensing, and resistivity data in GIS (Selvarani et al. 2016), influence factor (Selvam et al. 2015; Magesh et al. 2012), statistical methods (Falah et al. 2017), analytical hierarchy process (Dar et al. 2020; Saranya and Saravanan 2020) and GW modelling (Sashikkumar et al. 2017) were used in delineation of GWPZs. Clark and Fritz (1997) reported the use of isotopes of hydrogen (^{2}H and ^{3}H) and oxygen (^{18}O) in GW studies and assessment of its dynamics at basin level. In India, stable isotopes studies were also conducted in the GW recharge studies (Shivanna et al. 2004; Saha et al. 2013). Lee and Lee (2011) developed decision tree model to study the vulnerability to GW and changes happening in environmental parameters like temperature and rainfall patterns. However, the techniques of satellite remote sensing, and GIS have been adopted widely in identification, and mapping of GWPZs through integration of thematic database on topography, soils, lithology, drainage patterns, and lineaments (Nayak et al. 2017; Mokadem et al. 2018; Şener et al. 2018). In the recent years, probabilistic models were also being used in modelling and mapping of GWPZs through 'multi-criteria decision analysis' and modelling of weights-of-evidence (Mousavi et al. 2017; Sahoo et al. 2017). The machine-learning models like decision tree algorithms, fuzzy logic, and numerical modelling were also widely used in modelling of GWP and reported better results than the conventional methods (Barzegar et al. 2018; Golkarian et al. 2018). Rana et al. (2018) and Sharma et al. (2020) performed Hierarchical Cluster Analysis (HCA) to identify the GW pollution zones in Himachal Pradesh, India. Many studies have been conducted using remotely sensed datasets, geophysical surveys, and GIS in mapping of GWPZs (Pradhan 2009; Bera and Bandyopadhyay 2012; Magaia et al. 2018).

The GIS-based advance models like Frequency Ratio (FR) model (Naghibi et al. (2014), and Index of Entropy (IoE) (Al-Abadi and Shahid 2015), were sucessfully demonstrated in modelling, and assessment of GWPZs. By using FR model, the relationship between the independent, and dependent variables was assessed through adopting 'multi-layer integration of thematic maps' in GIS (Oh et al. 2011). The FR and logistic regression models provide flexible techniques in identification of GWPZs (Ozdemir 2011). Recently, FR model was tested in observation of the statistical trends in large datasets (Ding et al. 2017; Hong et al. 2017; Siahkamari et al. 2018) including identification of GWPZs (Mousavi et al. 2017; Sahoo et al. 2017). The GW entropy explains the effect of various GW controlling factors in determining its potential. It could be effectively used in computation of index system weights (Jaafari et al. 2014), demarcating the GWPZs, and their yields (Naghibi et al. 2014; Hou et al. 2017; Khoshtinat et al. 2019). Since GW is the main source for irrigation, domestic, and industrial use in semi-arid regions, accurate assessment and identification of GWPZs using advance techniques assume a greater importance. So far, the literature on integration of high-resolution satellite data, GIS, and bivariate statistical models (BSM) is limited in GWPZs mapping especially in hard rock terrains. Therefore, it is imperative to delineate the GWPZs by using advance remote sensing, GIS, and BSM for exploration and increase the water availability and control its scarcity in hard rock terrains of semi-arid regions. Hence, the core objective of the study is to model and delineate the GWPZs by using high resolution Sentinel-2 data and GIS by applying BSM of FR, and IoE models in Sarabanga Watershed (SBW) of Salem district, Tamil Nadu (TN) state, southern India. The comparative, and sensitivity analysis of BSM were also performed to assess the degree of influence of input parameters in precisely identification of GWPZs.

Study area

The SBW lies in southwest (SW) part of Salem district, TN state of southern India, and covers five tehsils, namely Omalur, Mettur, Edappadi, Yercaud and Sankari. It extends between 11° 29′ 27.72″ and 11° 56′ 5.15″ in northern latitudes and 77° 44′ 9.73″ to 78° 13′ 39.2″ in eastern longitudes and covers about 1175.3 sq. km (Fig. 1). Sarabanga river originates on the western slope of Shevaroy hills at 1630 m of above mean sea level (MSL) and flows through Omalur, Tharamangalam, Edappadi, and Thevur tehsils before joining the Cauvery river nearby by Bhavani town. The elevation ranges from 154 to 1641 m above MSL, and it rises from SW to northeast (NE). The SBW receives 800 to 1600 mm mean annual rainfall (MAR) during SW monsoon season, and it progressively increased towards the northern, north-eastern and eastern sections of the SBW with maximum at Yercaud hill region (1594.3 mm) (Arulmozhi and Arulraj 2017). Geologically, hornblende-biotite gneisses, charnockite, and granites represent hard consolidated Archaean crystalline rocks, which are the prominent formations of SBW. These formations are associated with recent alluvial, and colluvial deposits along the river channels,

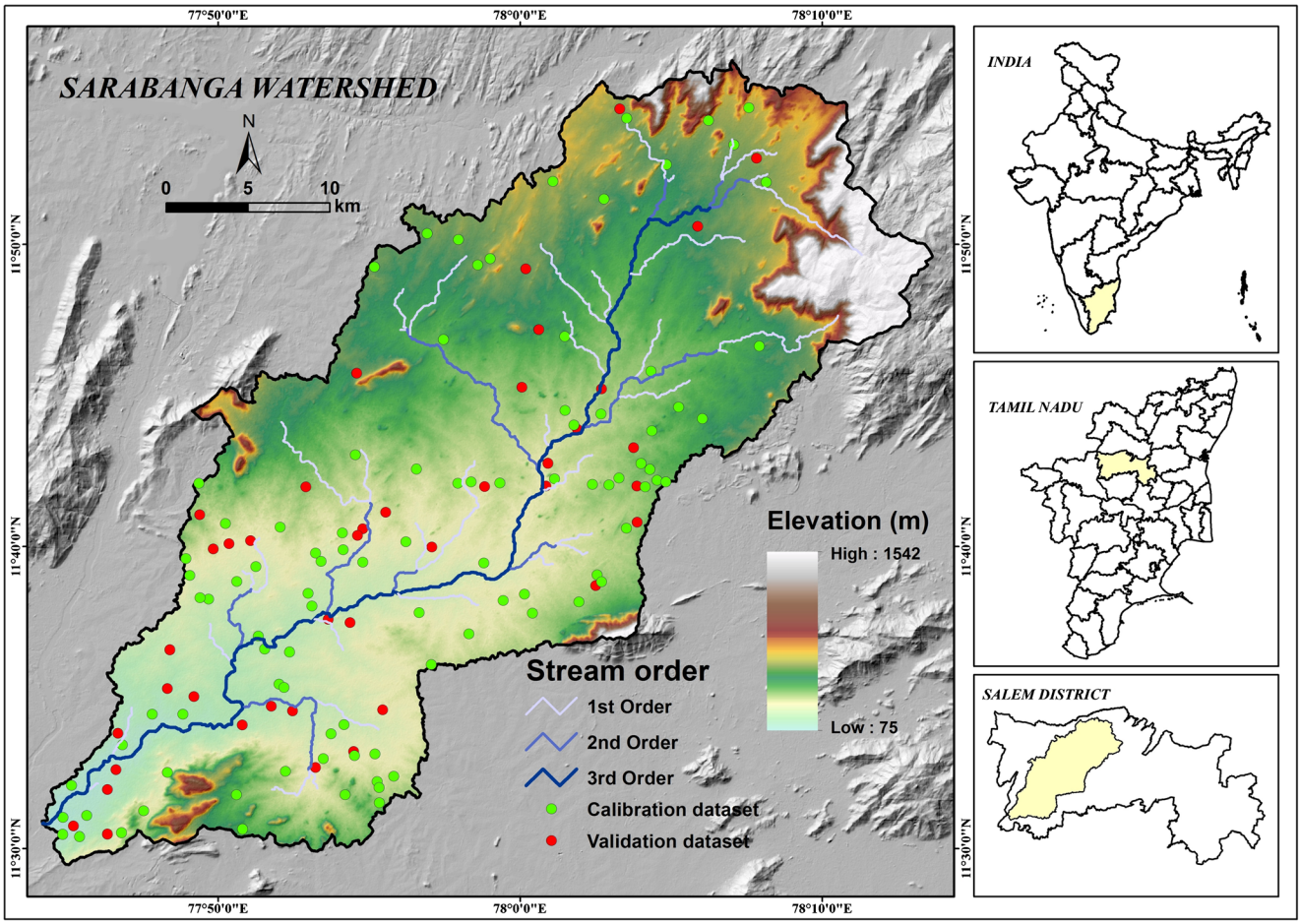

Fig. 1 Location map of the study area

and foothills. However, Quaternary alluvium is the prominent geological formation along the main course of Sarabanga river. The fractured crystalline rocks, and the recent colluvial deposits are the prominent aquifer systems in SBW with weathered thickness zone ranges from 1 to 25 m. GW occurrence mainly confined to weathered mantle in the fractured zones. These rocks are porous, and permeable, which are associated with secondary openings of fractures. The thickness of aquifer systems in SBW vary from 15 to 60m. In the toposequence of SBW, recharge mainly takes place in confined aquifers in the uplands, whereas, recharge-discharge together occur in the unconfined to semi-confined aquifer of midland areas. However, discharge takes place predominantly along the unconfined aquifers of the lowland areas. Major agriculture crops grown are paddy, groundnut, fodder, and sugarcane.

Materials and methods

Datasets used

Sentinel-2A multi-spectral instrument (MSI) data (10m) of 3rd March 2018 (tiles of T43PHP, T43PGN and T43PHN) from Copernicus Open Access Hub, and Digital Elevation Model (DEM) (12.5m) from 'Advanced Land Observing Satellite (ALOS) PALSAR' were acquired. The lineament data at 1:50,000 scale was derived from ISRO Bhuvan portal. The data on geology, and geomorphology at 1:250,000 scale was derived from the Bhukosh portal of 'Geological Survey of India (GSI)' for the watershed area and revised by using high-resolution Sentinel-2A and ALOS DEM datasets. The rainfall data of 30 years (1989 to 2018), acquired from the 'State Surface and Groundwater Resources Data Centre (SSGRDC)', Chennai, for 14 rain-gauge stations spread across the watershed. The data on soil parameters at 1:50,000 scale was acquired for the watershed from the 'Tamil Nadu Agricultural University (TNAU)'. The input parameters used in the spatial modelling of GWPZs are depicted in Table 1.

Georeferenced well inventory data

GIS-based well locations mapping was conducted to establish the relationship among the geological, geomorphological, and GW characteristics of wells to validate the identified GWPZs (Haghizadeh et al. 2017). Firstly, field survey was

Table 1 Various input datasets and their characteristics

Sl. no	Dataset	Input variables	Temporal coverage	Spatial resolution	Source
1	Sentinel-2A	LU/LC	16 days	10 m	https://scihub.copernicus.eu/
2	ALOS PALSAR DEM	Slope, drainage density	-	12.5 m	https://asf.alaska.edu/
3	Lineament	Lineament density	-	1:50,000	http://bhuvan.nrsc.gov.in
4	Geology Geomorphology	Geology Geomorphology	-	1:250,000	http://bhukosh.gsi.gov.in/
5	Rain gauge data	Rainfall	1989–2018	-	State Surface and Groundwater Resources Data Centre (SSGRDC)
6	Soil	Texture	-	1:50000	Tamil Nadu Agricultural University (TNAU)

conducted to identify, and map the 135 well locations distributed throughout the watershed under different geological formations by using hand-held 'Global Positioning System (GPS)' (Fig. 1). Out of 135 well locations, 94 wells (70%) and 41 wells (30%) were arbitrarily grouped as calibration, and validation datasets, respectively. The 'calibration dataset' was used in spatial modelling and delineation of GWPZs, whereas the 'validation dataset' was used to validate the GWPZs, and accuracy assessment of models adopted. The calibrated dataset of well locations was superimposed on all contributing factor maps in GIS to understand their interrelationship.

Computation of groundwater conditioning factors

GWPZs mapping can be carried out by investigating the controlling factors on GW storage and occurrence (Tolche 2020). GW occurrence is determined by many parameters like rainfall, elevation, geology, geomorphology, slope, drainage density (Dd), lineament density (Ld), type of soil, land use/land cover (LU/LC), recharge potential, aquifer transmissivity, and anthropogenic activities (Paul et al. 2020). However, in the current investigation, eight major contributing factors, which includes geology, geomorphology, Dd, Ld, slope, soil texture, rainfall, and LU/LC were used for the identification of GWPZs. The thematic raster database for the input factors were developed in ArcGIS at 10m × 10m grid cell by using 'polygon to raster conversion tool' for their integrated analysis and mapping of GWPZs by adopting FR and IoE models.

The distinct LU/LC classess of the SBW was generated through digital interpretation of Sentinel-2A data by using 'supervised classification algorithm' in ArcGIS. The watershed boundary, and drainage network were generated through analysis of high-resolution ALOS DEM (12.5m) by using 'ArcHydro' tool in ArcGIS to compute 'Dd'. The slope classes were computed from ALOS DEM by using 'slope tool' in ArcGIS. With the help of derived lineaments, the 'Ld' was computed to define its density in the given unit area. The 'Inverse Distance Weighted (IDW)' interpolation technique was used to develop the rainfall raster by considering the 30 years rainfall data (1989 to 2018) of 14 rain-gauge stations. The soil texture map was developed in GIS by using the legacy soil data at 1:50,000 scale and the same used in the spatial modelling.

Building of BSMs

FR model was adopted to establish the probabilistic correlation between dependent (groundwater), and independent (conditioning) factors (Oh et al. 2011; Naghibi et al. 2016). The model has robustness in execution and understands the derived results (Khosravi et al. 2018; Khoshtinat et al. 2019). FR model was adopted to determine the effect of individual conditioning factors to identify the GW occurrence. FR model was expressed as follows;

$$FR = \frac{W/TW}{CP/TP} \quad (1)$$

where W explains the 'total pixels of wells' for the given class of input; TW denotes the 'total pixels of well', whereas, CP explains the 'total pixels' in the given thematic class and TP indicates the 'total pixels'. To find out the GWP, the FR value of 'each class in the given parameter' was taken as the weight of the given class. Finally, the GWPZs were computed as (Jaafari et al. 2014; Naghibi et al. 2014):

$$GWPZ = \sum_{i=1}^{n} FR_i \quad (2)$$

where FR_i denotes the 'frequency ratio of a factor' and n explains the 'total number of input factors'. The spatial association between the contributing factors of GW and the occurrence of GWPZs was analysed by using the FR model (Table 3). The FR values were determined by using Eq. (1), where the average of the proportion of the 'area of wells' to 'the entire watershed' is assumed as 1 (Moghaddam et al. 2015). If the FR is larger than 1, it indicates high correlation, and if it is <1, it shows the low correlation (Oh et al. 2011).

In IoE model, the entropy explains the 'degree of uncertainty' in the given random variable (Ihara 1993). The entropy of model shows the 'degree of variability' and unreliability of

a model (Yufeng and Fengxiang 2009). The following mathematical expressions were used to determine the coefficient of information (Jaafari et al. 2014):

$$P_{ij} = FR = \frac{b}{a} \tag{3}$$

$$(P_{ij}) = \frac{P_{ij}}{\sum_{j=1}^{sj} P_{ij}} \tag{4}$$

$$H_j = -\sum_{i=1}^{Sj} (P_{ij}) \log_2 (P_{ij}), \quad j = 1, \ldots, n \tag{5}$$

$$H_{jmax} = \log_2 Sj \tag{6}$$

$$I_j = \frac{H_{jmax} - H_j}{H_{jmax}}, \quad I = (0, 1), \quad j = 1, \ldots, n \tag{7}$$

$$w_j = I_j P_{ij} \tag{8}$$

where (P_{ij}) denotes the 'probability density', whereas, H_j and H_{jmax} explains the 'entropy values', Sj indicates the 'total number of classes', I_j is the 'information coefficient' and wj is the 'resultant weight' of the factor. The values of wj range between 0 and 1. The derived GWPZs were assessed by using Eq. 9:

$$GWPZ = \sum_{i=1}^{n} FR_i \times w_j \tag{9}$$

where FR_i denotes the 'frequency ratio of a factor' and wj is the 'resultant weight' of the factor as a whole.

Validation and sensitivity analysis of BSMs

In any predictive modelling, assessment of its performance, validation and uncertainty is essential (Dar et al. 2020). Many researchers were used 'Area Under the Curve-Receiver Operating Characteristic' (AUC-ROC) to assess the accuracy of delineated GWPZs (Nhu et al. 2020; Naghibi et al. 2016; Rahmati et al. 2015). FR, and IoE models were validated by adopting AUC-ROC to determine the degree of the existence or non-existence of GW (Rahmati et al. 2016). To evaluate the influence of contributing factors, and sensitivity of models, a performed Variable Importance Analysis (VIA) was performed. It represents the statistical significance of each contributing factor with respect to its effect on the generated model (Wei et al. 2015). The regression technique of random forest model was used to measure the variable importance of outputs of FR, and IoE models and explain the importance of each of the input variables. The detailed methodology followed is shown in Fig. 2.

Results and discussion

The analysis shows that SBW is predominantly underlined by hornblende-biotite gneisses (64.4%), charnockite (23.2%) in northern regions of the watershed and granites (7.6%) in Pudupalayam village as isolated outcrops surrounded by charnockite (Table 2 and Fig. 3a). The geomorphologic features are base to understand the structural features, parent material, and lithological formations in determining the GWP especially in hard rock terrains (Rao et al. 2000). Analysing the nature, and extend of geomorphologic units immensely helped in delineating the GWPZs (Arulbalaji et al. 2019). In the watershed, seven distinct geomorphologic units namely structural hills (0.54%), dissected hills (10.27%), residual hills (1.15), linear ridges (0.7%), pediments (15.8%), pediplain (60.5%), and upper valley (8.8%) were identified (Table 2 and Fig. 3b). The structural hills, dissected hills, and residual hills are developed in north, south, and at places in eastern parts of the watershed, which are normally unfavourable for GW occurrence (Kumar et al. 2020). The 'moderately weathered pediplain' with medium to coarse gravel are quite common in the watershed. The pediments are distinguished by moderately steep topography spreading below the hilly regions associated with low permeability and GWP (Rajaveni et al. 2015). The linear ridges associated with barren lands noticed in the eastern regions of Sarabanga river. However, the isolated 'residual hills' with steep slopes and rounded in nature were noticed in the northern parts of watershed.

'Dd' explains the proximity of the drainage channels in the given unit area (Horton 1932). It has direct relationship with the permeability (Agarwal et al. 2013; Kanagaraj et al. 2019), slope, geomorphological, and LU/LC conditions of the terrain (Paul et al. 2020); hence, it was considered as an important parameter in identification of GWPZs. GIS-based techniques are being widely applied in delineation of drainage channels and computation of 'Dd' in hydrological models (Reddy et al. 2018). The lower 'Dd' indicates the porous soil, thick vegetation cover and low relief, whereas, the higher 'Dd' implies the opposite scenario (Reddy et al. 2002). The 'Dd' of watershed was categorized as very low (<1.5 km/km^2), low (1.5 to 2.5 km/km^2), moderate (2.5 to 3.5 km/km^2), high (3.5 to 4.5 km/km^2), and very high (>4.5 km/km^2) (Table 2 and Fig. 3c). Lineaments originate through the structural/tectonic process with secondary porosity have significant contribution in GW accumulation (Suganthi et al. 2013) and exploration (Şener et al. 2018). 'Ld' in the SBW ranges from 0 to 3.8 km/km^2 and further classified into five sub-categories, i.e. 0 to 1 km/km^2, 1 to 1.5 km/km^2, 1.5 to 2 km/km^2, 2 to 2.5 km/km^2 and >2.5 km/km^2, respectively (Table 2 and Fig. 3d).

As slope significantly influences the surface runoff, it was considered an important criterion in identification of GWP (Patra et al. 2018). As per the slope criteria defined by Singh et al. (2016), nine slope classes, i.e. 0 to 1% (level to nearly level), 1 to 3% (very gently sloping), 3 to 5% (gently sloping), 5 to 10% (moderately sloping), 10 to 15% (moderately steeply sloping), 15 to 25% (steeply sloping), 25 to 33% (very steeply

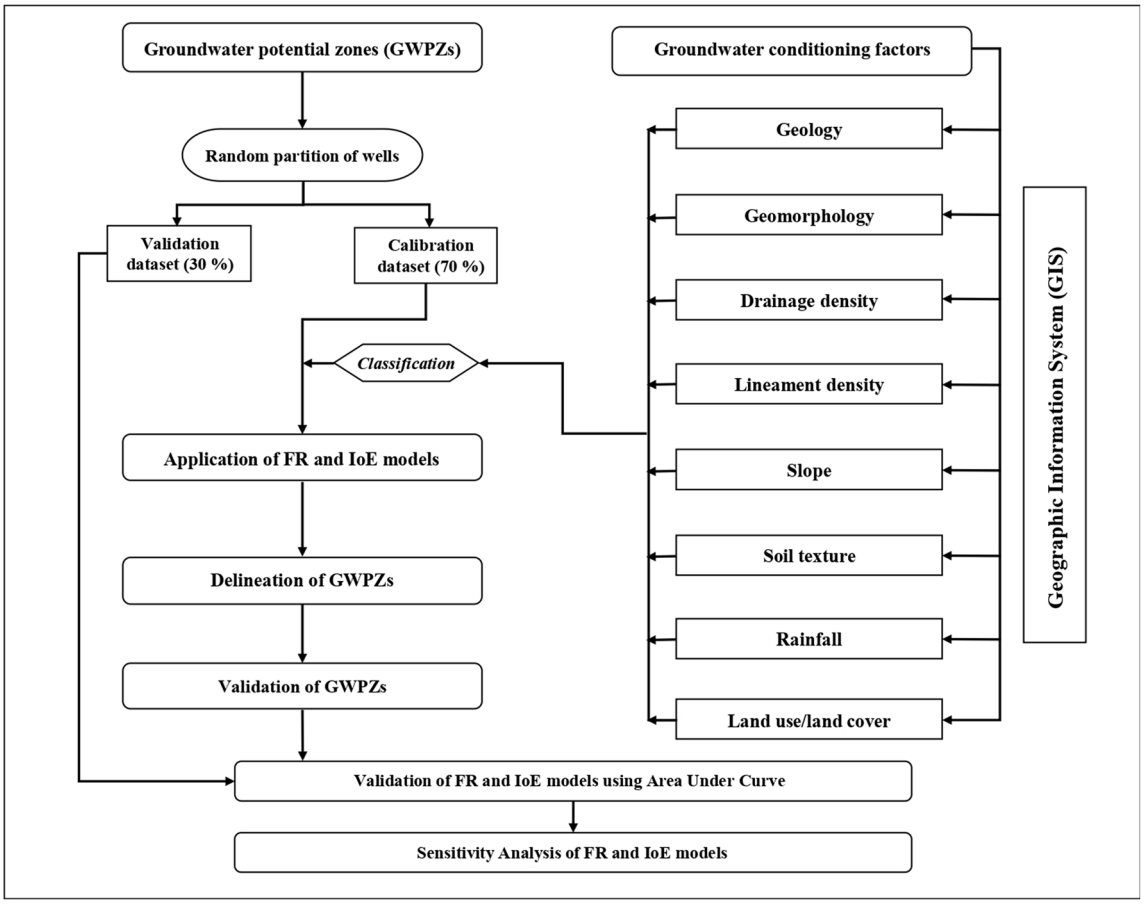

Fig. 2 Methodology followed in the study

sloping), 33 to 55% (strongly sloping), and above 50% (very strongly sloping), were identified. Very gentle (31.9%) to gentle slopes (25.9%) are the dominant classes in SBW (Table 2 and Fig. 3e). Soil texture determines water infiltration that affects the recharge, occurrence, and circulation of GW (Das 2017). Hence, the soil texture was considered as an important contributing factor in estimating infiltration rates (Lee and Lee 2015) and identification of GWPZs. In SBW, eight distinct soil textural classes, i.e. sandy clay loam, sandy loam, loamy sand, clay loam, sandy clay, clay, silty clay, and loam, were identified (Table 2 and Fig. 3f). Sandy clay loam soils are dominant soil textural classes with an area of 448.4 sq.km (38.1%), whereas, sandy loam and sandy clay soils covered 315.5 (26.8%) and 117.6 (10%) sq.km, respectively.

The amount, intensity, and distribution of rainfall play an important role in GW recharge and determine the GWP depending upon the hydrogeological characteristics of the terrain (Shi et al. 2016). Since, rainfall varies with time and space, it is essential to ascertain the role of rainfall in identification of GWPZs (Patra et al. 2018). The SBW receives 800 to 1600 mm Mean Annual Rainfall (MAR), and the maximum amount of rainfall was received during the SW monsoon season. It was reclassified into six classes, i.e. < 350 mm/year, 350 to 450 mm/year, 450 to 550 mm/year, 550 to 650 mm/year, 650 to 750 mm/year, and > 750 mm/year (Table 2 and Fig. 3g). The LU/LC pattern influences the GWP, and infiltration rate of water through soil (Singha et al. 2019). In the watershed, nine LU/LC classes, namely single crop, double-crop, current fallows, degraded forest, deciduous forest, scrublands, wastelands, settlements, and waterbodies were identified through interpretation of Sentinel-2A satellite data. The single crop is predominantly covered with 410.8 sq.km (35%), while forest land covered approximately 147.9 sq.km (12.6%) of the area (Table 2 and Fig. 3h).

Assessment of GWPZs using FR model

The analysis shows that the classes of LU/LC layer like double crop, single crop, and settlements classes have high FR values of 1.26, 1.2 and 1.8, respectively, which indicates the favourability of these classes for occurrence of GW. In case of Dd, the classes such as 1.5 to 2.5 km/km^2 and 3.5 to 4.5 km/km^2 have higher FR values of 1.5 and 1.3, respectively, and it indicates their higher influence on GW occurrence. The terrain with slope <1 % shows the highest value of FR (1.8), whereas the terrain with 1 to 3 % slope shows the FR value of 0.9 and 3 to 5% shows 1.3. However, the lowest value of FR of 0.7 was

Table 2 FR and IoE model values of groundwater conditioning factors

Conditioning factor	Class	Area (pixels)	Area % (a)	Wells (No.)	Wells % (b)	FR (b/a)	(P_{ij})	H_j	H_{jmax}	I_j	W_j
Geology	Amphibolite	14,098	0.12	1	1.06	8.87	0.62	1.52	1.05	0.52	0.12
	Charnockite	2,726,230	23.2	8	8.51	0.37	0.03				
	Dunite	55,154	0.47	1	1.06	2.27	0.16				
	Dunite-pyroxenite	56,369	0.48	0	0	0	0				
	Fissile hornblende-biotite gneisses	7,564,105	64.36	74	78.72	1.22	0.09				
	Fuchsite quartzite	22,179	0.19	0	0	0	0				
	Granite	897,948	7.64	9	9.57	1.25	0.09				
	Syenite	403,212	3.43	1	1.06	0.31	0.02				
	Laterite	13,705	0.12	0	0	0	0				
Geomorphology	Structural hills	62,976	0.54	0	0	0	0	1.47	1.05	0.47	0.11
	Dissected hills	1,206,996	10.27	0	0	0	0				
	Residual hills	134,952	1.15	0	0	0	0				
	Linear ridges	81,821	0.7	0	0	0	0				
	Pediments	1,853,609	15.77	13	13.83	0.88	0.27				
	Pediplain	7,112,845	60.52	72	76.6	1.27	0.39				
	Upper valley	1,034,229	8.8	9	9.57	1.09	0.34				
	Mining area	96,508	0.82	0	0	0	0				
	Waterbodies	169,064	1.44	0	0	0	0				
Drainage density (Dd)	<1.5	6,930,020	58.96	55	58.51	0.99	0.2	1.67	1.43	0.67	0.13
	1.5–2.5	1,463,856	12.46	17	18.09	1.45	0.29				
	2.5–3.5	1,211,852	10.31	7	7.45	0.72	0.15				
	3.5–4.5	1,057,038	8.99	11	11.7	1.3	0.26				
	>4.5	1,090,234	9.28	4	4.26	0.46	0.09				
Lineament density (Ld)	<1	8,650,967	73.61	68	72.34	0.98	0.2	1.69	1.43	0.69	0.13
	1–1.5	1,092,170	9.29	12	12.77	1.37	0.28				
	1.5–2	607,613	5.17	5	5.32	1.03	0.21				
	2–2.5	506,442	4.31	3	3.19	0.74	0.15				
	>2.5	895,808	7.62	6	6.38	0.84	0.17				
Slope	<1	1,852,289	15.76	26	27.66	1.76	0.38	1.58	1.05	0.58	0.12
	1–3	3,755,158	31.95	27	28.72	0.9	0.2				
	3–5	3,043,919	25.9	31	32.98	1.27	0.28				
	5–10	1,834,903	15.61	10	10.64	0.68	0.15				
	10–15	360,916	3.07	0	0	0	0				
	15–25	514,553	4.38	0	0	0	0				
	25–33	265,230	2.26	0	0	0	0				
	33–50	121,681	1.04	0	0	0	0				
	>50	4351	0.04	0	0	0	0				
Soil texture	Sandy clay loam	4,484,501	38.16	34	36.17	0.95	0.13	1.75	1.05	0.75	0.14
	Sandy loam	3,153,779	26.83	25	26.6	0.99	0.13				
	Loamy sand	651,996	5.55	6	6.38	1.15	0.16				
	Clay loam	683,798	5.82	12	12.77	2.19	0.3				
	Sandy clay	1,176,328	10.01	8	8.51	0.85	0.12				
	Clay	903,860	7.69	9	9.57	1.24	0.17				
	Silty clay	4502	0.04	0	0	0	0				
	Loam	5961	0.05	0	0	0	0				
	Others	688,275	5.86	0	0	0	0				
Rainfall	<350	1,161,640	9.88	12	12.77	1.29	0.24	1.57	1.29	0.57	0.12

Table 2 (continued)

Conditioning factor	Class	Area (pixels)	Area % (a)	Wells (No.)	Wells % (b)	FR (b/a)	(P_{ij})	H_j	H_{jmax}	I_j	W_j
	350–450	1,110,216	9.45	17	18.09	1.91	0.36				
	450–550	3,264,687	27.78	40	42.55	1.53	0.29				
	550–650	5,664,786	48.2	25	26.6	0.55	0.1				
	650–750	362,045	3.08	0	0	0	0				
	>750	189,626	1.61	0	0	0	0				
LU/LC	Double crop	3,863,630	32.87	39	41.49	1.26	0.21	1.68	1.05	0.68	0.13
	Single crop	4,107,995	34.95	39	41.49	1.19	0.2				
	Current fallows	779,304	6.63	2	2.13	0.32	0.05				
	Wastelands	830,764	7.07	9	9.57	1.35	0.23				
	Scrub lands	95,723	0.81	0	0	0	0				
	Degraded forest	134,502	1.14	0	0	0	0				
	Deciduous forest	1,480,227	12.59	1	1.06	0.08	0.01				
	Settlements	279,246	2.38	4	4.26	1.79	0.3				
	Waterbodies	181,609	1.55	0	0	0	0				

found with slope class of 5 to 10%. In SBW, it was noticed that as slope gradient increases, the FR value decreases. The Ld between 2 and 2.5 km/km^2 shows the FR value of 0.8, and it indicates very less probability of GW occurrence, whereas the Ld between 1 and 1.5 km/km^2 shows the ratio of 1.4 and it indicates a high probability. In geomorphology layer, the highest FR values were found in the pediplain (1.3); similarly, the next highest values were noticed in the upper valley (1.1), and pediments (0.9), which indicate the relationship of geomorphologic structures and the GW occurrence. As far as geology is concern, the higher FR values are allied with amphibolite, dunite, granite, and fissile hornblende-biotite gneisses with FR equal to 8.9, 2.3, 1.3 and 1.2, respectively; it shows their higher potential for occurrence of GW. The rest of the geological classes with zero FR values denote the low possibility of GW occurrence. The FR values are high for clay loam (2.2), clay (1.3), and loamy sand (1.2) classes and relatively low for the remaining texture classes. The higher FR values indicate the higher infiltration rates of the textural classes. When the infiltration rate accelerates the GW, it contributes the higher recharge conditions. In SBW, the relationship between the rainfall and GWP shows 350 to 450 mm/year (2.0), 450 to 550 mm/year (1.6) and <350 mm (1.3); these positive FR values explains the local topographic conditions. The areas with high rainfall discharges associated with Yercaud hills with steep slopes, and sparse forest cover reduce the likelihood of water infiltration. The final GWPZs were delineated by applying FR model (Eq. 2) with the hypothesis that all the input GW variables have uniform influence on the occurrence of GWP (Fig. 4a). The obtained GWPZs values are in range of 3.91 to 67.29, which were classified based on mean and standard deviation (SD) classification scheme into five classes: very poor (< 13.1), poor (13.05 to 21.64), good (21.64 to 30.23), very good (30.23 to 38.82), and excellent (> 38.82). The very poor to poor classes encompass an area of 15.41 % (181.17 km^2); the good and very good classes extend over an area of 75.23 % (884.18 km^2), while the area under excellent class occupies only 9.36 % (109.95 km^2) (Table 3).

Assessment of GWPZs using IoE model

The results attained on application of IoE model in assessment of GWPZs are shown in Table 3. The computed weights for geomorphology, geology, LU/LC, Dd, slope, and Ld are 0.11, 0.12, 0.13, 0.13, 0.12, and 0.13, respectively. Similarly, for soil texture, the weight is 0.14, and for the rainfall parameter, the weight is 0.12. The final GWPZs map developed by using IoE model was shown in Eq. 9. The obtained GWPZs values are ranges from 3.49 to 27.47. Based on mean and SD, they were classified into five classes, i.e. very poor (< 8.67), poor (8.67 to 12.23), good (12.23 to 15.89), very good (15.89 to 19.35), and excellent (> 19.35) as shown in Fig. 4b. The very poor to poor classes encompass an area of 15.55 % (182.71 km^2); the good and very good classes extend over an area of 75.08 % (882.47 km^2), while the excellent class occupies 9.37 % (110.12 km^2). The very good, and excellent classes are concentrated mainly in SE part of the watershed (Table 3).

Validation of FR and IoE models

The critical stage of any modelling is validation, in the absence of this, models depict less scientific value (Nampak et al. 2014). The AUC-ROC was adopted to validate the input models prediction rate (Pourghasemi et al. 2012; Tehrany

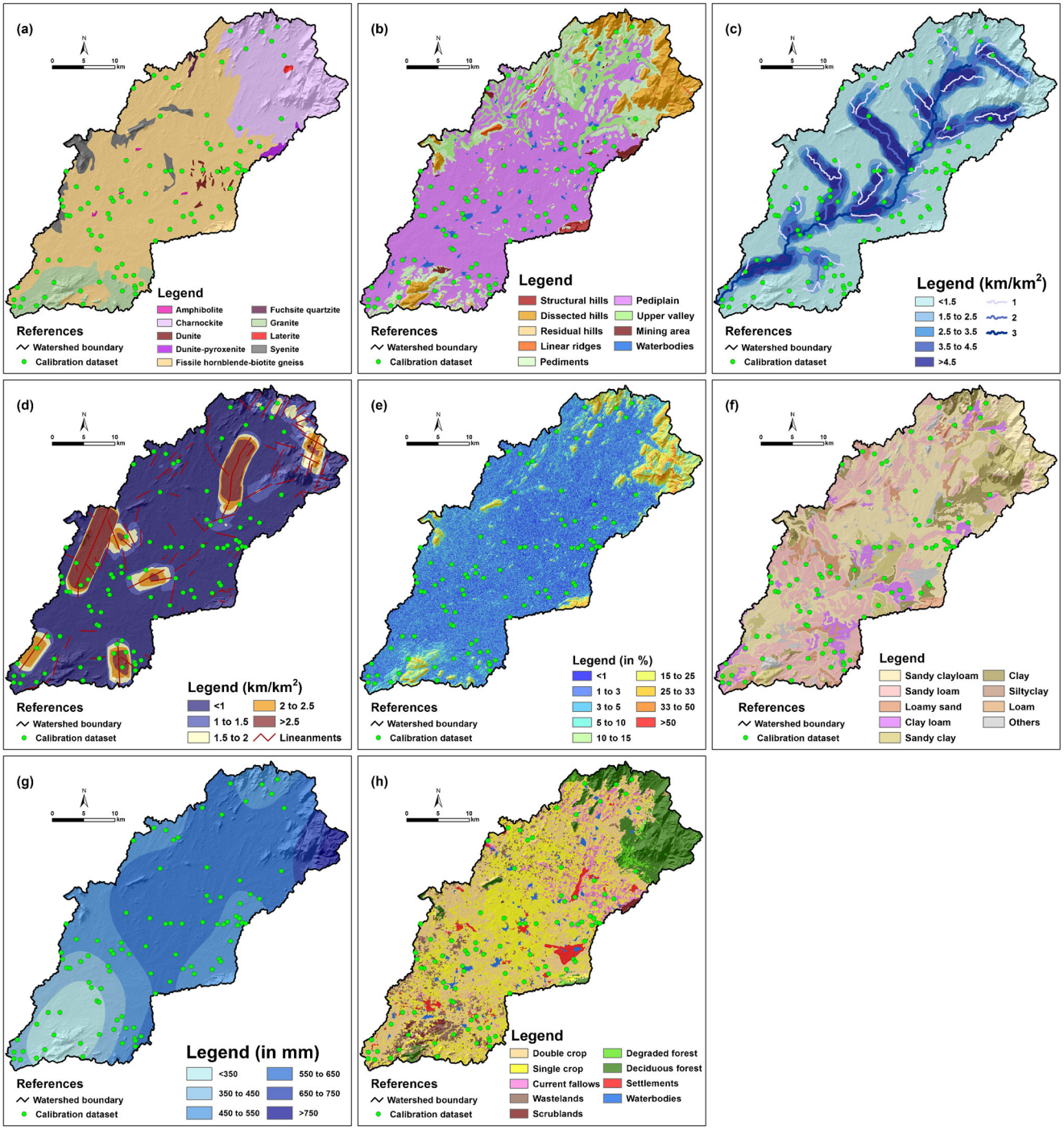

Fig. 3 Contributing parameters in modelling of GWPZs: (a) Geology, (b) Geomorphology, (c) Drainage density (Dd), (d) Lineament density (Ld), (e) Slope, (f) Soil texture, (g) Rainfall, and (h) LU/LC

et al. 2017). The AUC-ROC values were estimated through comparison of GW depth of wells collected through field surveys with GWPZs derived from FR and IoE models. The quantitative inter-relation lies among the model predictions, and AUC-ROC were grouped into five categories: excellent (0.9–1), very good (0.8–0.9), good (0.7–0.8), average (0.6–0.7), and poor (0.5-0.6). The AUC-ROC values were estimated for FR and IoE models by using GW depth of 41 validation wells, and it shows 0.7313 and 0.7084, respectively (Fig. 5). The accuracy assessment of the models indicates that the adopted two models yield good estimation; however, FR model depicted relatively higher estimation than the IoE model. The study clearly demonstrates that BSM can be effectively applied as a realistic and simple method in modelling and evaluating the GWP. The strengths of BSM are simple in implementation and provide reasonable accuracy in spatial

Table 3 Area under different GWPZ's derived from FR and IoE models

GWPZs	FR model		IoE model	
	Area (sq.km)	Area (%)	Area (sq.km)	Area (%)
Excellent	110.0	9.4	110.1	9.4
Very good	686.2	58.3	665.8	56.7
Good	198.0	16.9	216.8	18.4
Poor	75.5	6.4	87.4	7.4
Very poor	105.7	9.0	95.3	8.1

prediction, with the potential to distinguish the input factors or combinations of input factors in the evaluation of GWP (Khoshtinat et al. 2019).

Sensitivity analysis

Sensitivity analysis performed through VIA shows that out of the eight input contributing factors, the geology, slope, and rainfall are the three important factors, which significantly contribute in identification of GWPZs through FR model. In other words, the biotite genesis, and dunite-pyroxenite formations with slope less 3% and rainfall ranging from 550 to 750mm influence more in identification of GWPZs (Fig. 6a). In IoE model, drainage density, slope and rainfall found to be three important influencing factors, in identification of GWPZs (Fig. 6b). The low land regions with slope less 3% and rainfall ranging from 550 to 750mm was found to be more contributing in identification of GWPZs. Besides geology, slope, rainfall and Dd, the other contributing factors like geomorphology, and soil texture especially the areas under pediplain associted with sandy loam, and sandy clay have their own contribution in GW recharge, and identification of GWPZs.

Conclusions

In the study, geology, geomorphology, Dd, Ld, slope, soil texture, rainfall, and LU/LC were considered as major contributing factors in identification of GWPZs through GIS and BSM. The GWPZs were determined by adopting FR, and IoE models and established the relationships among the input GW conditioning factors. The study shows that both FR, and IoE models exhibited very good and good performance in modelling, and assessment of GWP, respectively, and explained the most critical classes in each conditioning factor. In comparison with IoE model, the FR model not only has better performance but also has simple procedure in its computation. The validation results confirm that the FR, and IoE models are ideal for assessing GWP, simulating the relationships between the GW occurrence and GW conditioning factors. The results

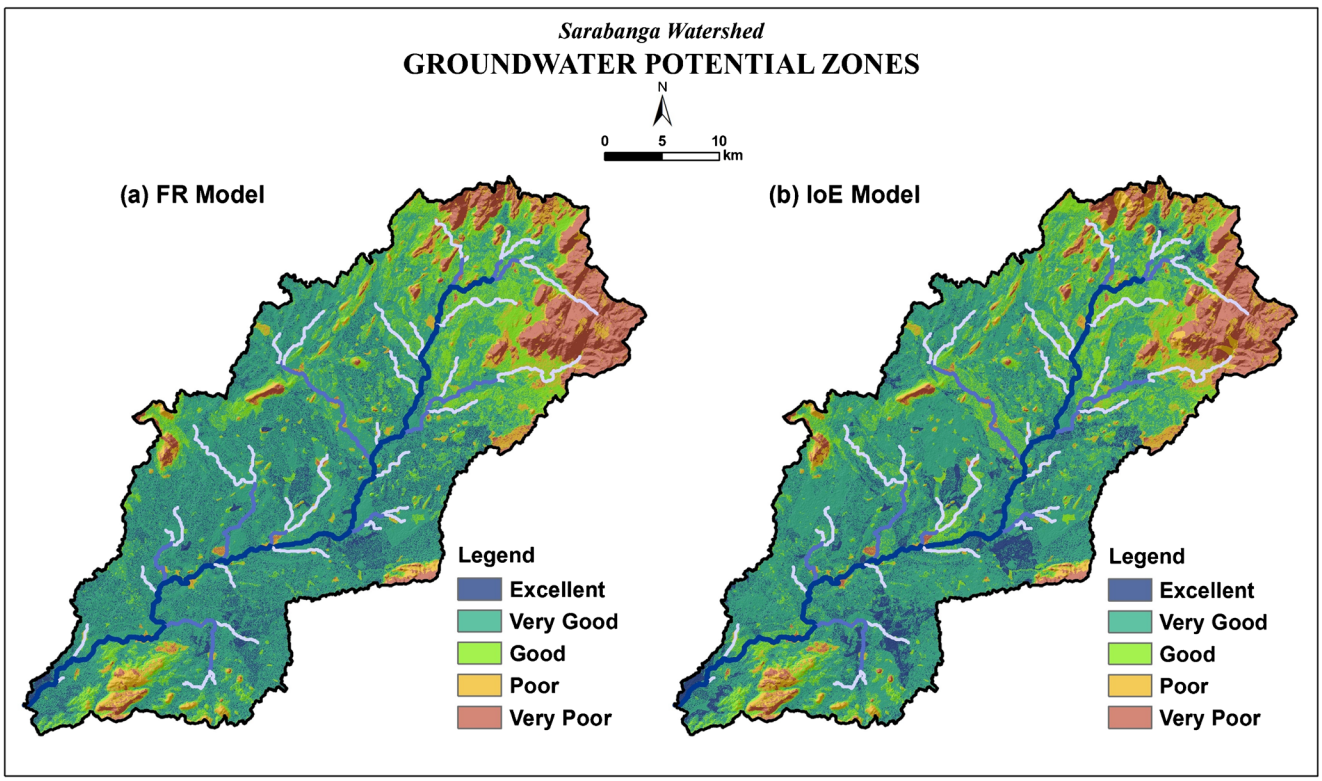

Fig. 4 GWPZs derived from **a** frequency ratio (FR) and **b** index of entropy (IoE) models

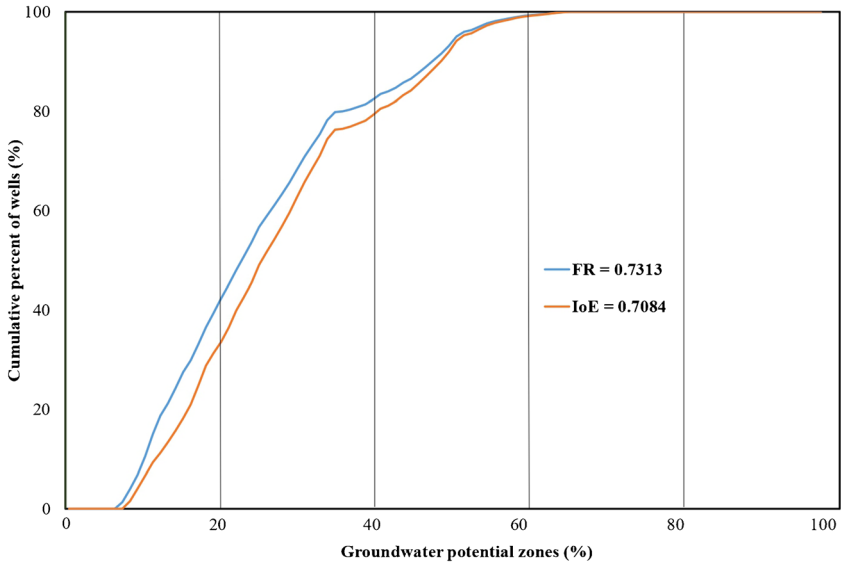

Fig. 5 Validation of FR and IoE models using AUC-ROC

obtained are immensely useful in systematic evaluation, development of GW exploration and environmental strategic plans by the government agencies and policymakers. Sensitivity analysis was carried out through VIA, and it

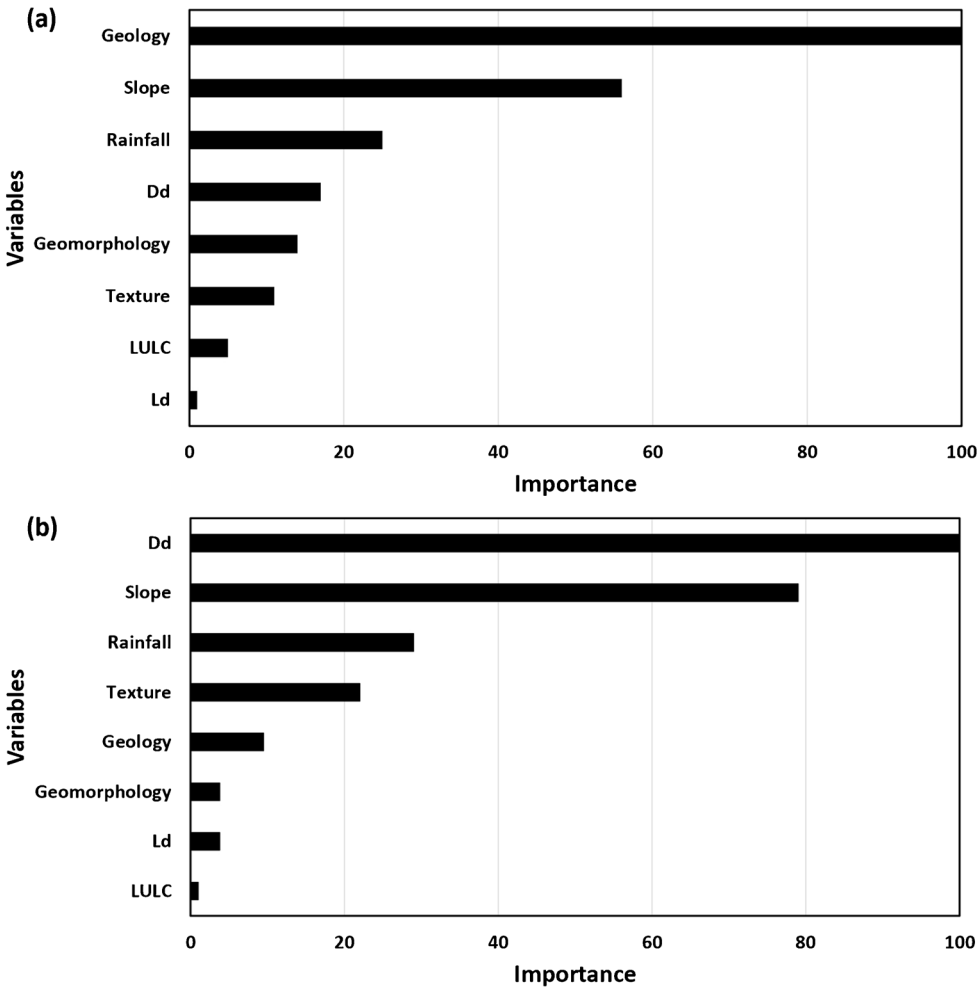

Fig. 6 Rank of variables by their importance. **a** frequency ratio (FR) and **b** index of entropy (IoE) models

indicates that in both FR, and IoE models, geology, slope, rainfall, and Dd found to be important influencing factors in identification of GWPZs. The study clearly demonstrates the potential of high-resolution Sentinel-2 data, and robustness of BSM in obtaining the accurate, reliable, and cost-effective results for effective GIS-based spatial modelling of GWPZs in hard rock terrain of semi-arid ecosystems.

Acknowledgements Authors of the article extend sincere thanks to the US Geological Survey (USGS) for open access of Sentinel-2 datasets of the study area. Authors also thank the Director, ICAR-National Bureau of Soil Survey and Land Use Planning, Nagpur, for extending the facilities in completion of the work. This research work did not receive any specific grant from funding agencies. We sincerely thank anonymous reviewers whose valuable comments and suggestions greatly helped to improve the overall quality of manuscript.

Declarations

Conflict of interest The authors declare no competing interests.

References

Agarwal R, Garg PK (2016) Remote sensing and GIS based groundwater potential and recharge zones mapping using multi-criteria decision-making technique. Water Resour Manag 30:243–260. https://doi.org/10.1007/s11269-015-1159-8

Agarwal E, Agarwal R, Garg RD, Garg PK (2013) Delineation of groundwater potential zone: an AHP/ANP approach. J Earth Syst Sci 122: 887–898. https://doi.org/10.1007/s12040-013-0309-8

Al-Abadi AM, Shahid S (2015) A comparison between index of entropy and catastrophe theory methods for mapping groundwater potential in an arid region. Environ Monit Assess 187(9):4801. https://doi.org/10.1007/s10661-015-4801-2

Arulbalaji P, Padmalal D, Sreelash K (2019) GIS and AHP techniques-based delineation of groundwater potential zones: a case study from Southern Western Ghats India. Sci Rep 9:2082. https://doi.org/10.1038/s41598-019-38567-x

Arulmozhi S, Arulraj GP (2017) Rainfall variation and frequency analysis study of Salem district Tamil Nadu. Indian J Geo-Mar Sci 46(01): 213–218

Barzegar R, Moghaddam AA, Deo R, Fijani E, Tziritis E (2018) Mapping groundwater contamination risk of multiple aquifers using multi-model ensemble of machine learning algorithms. Sci Total Environ 621:697–712. https://doi.org/10.1016/j.scitotenv.2017.11.185

Bera K, Bandyopadhyay J (2012) Groundwater potential mapping in Dulung watershed using remote sensing and GIS techniques, West Bengal, India. Int J Sci Res Publ 2:1–7

Chatterji PC, Singh S, Qureshi LH (1978) Hydro-geomorphology of the central Luni basin, western Rajasthan, (India). Geoforum 9(3):211–224. https://doi.org/10.1016/0016-7185(78)90011-8

Chen YN, Li Z, Fan YT, Wang HJ, Deng HJ (2015) Progress and prospects of climate change impacts on hydrology in the arid region of northwest China. Environ Res 139:11–19. https://doi.org/10.1016/j.envres.2014.12.029

Clark ID, Fritz P (1997) Environmental Isotopes in Hydrogeology. CRC Press

CWC and CGWB (2016) A 21st Century Institutional Architecture for India's Water Reforms. http://cgwb.gov.in/INTRA-CGWB/Circulars/Report_on_Restructuring_CWC_CGWB.pdf. Accessed 30th March 2020

Dar T, Rai N, Bhat A (2020) Delineation of potential groundwater recharge zones using analytical hierarchy process (AHP). Geol Ecol Landsc:1–16. https://doi.org/10.1080/24749508.2020.1726562

Das S (2017) Delineation of groundwater potential zone in hard rock terrain in Gangajalghati block, Bankura district, India using remote sensing and GIS techniques. Model Earth Syst Environ 3:1589–1599. https://doi.org/10.1007/s40808-017-0396-7

Ding Q, Chen W, Hong H (2017) Application of frequency ratio, weights of evidence and evidential belief function models in landslide susceptibility mapping. Geocarto Int 32:619–639. https://doi.org/10.1080/10106049.2016.1165294

Etikala B, Golla V, Li P (2019) Renati, S. Deciphering groundwater potential zones using MIF technique and GIS: a study from Tirupati area, Chittoor District, Andhra Pradesh, India. Hydro Research 1:1–7. https://doi.org/10.1016/j.hydres.2019.04.001

Falah F, Ghorbani Nejad S, Rahmati O, Daneshfar M, Zeinivand H (2017) Applicability of generalized additive model in groundwater potential modelling and comparison its performance by bivariate statistical methods. Geocarto Int 32:1069–1089. https://doi.org/10.1080/10106049.2016.1188166

FAO (2011) The state of the world's land and water resources for food and agriculture (SOLAW) – managing systems at risk. Food and Agriculture Organization of the United Nations, Rome and Earthscan, London, p 285

Golkarian A, Naghibi SA, Kalantar B, Pradhan B (2018) Groundwater potential mapping using C5.0, random forest, and multivariate adaptive regression spline models in GIS. Environ Monit Assess 190: 149. https://doi.org/10.1007/s10661-018-6507-8

Haghizadeh A, Moghaddam DD, Pourghasemi HR (2017) GIS-based bivariate statistical techniques for groundwater potential analysis (an example of Iran). J Earth Syst Sci 126(8):109. https://doi.org/10.1007/s12040-017-0888-x

Hong H, Chen W, Xu C, Youssef AM, Pradhan B, Tien Bui D (2017) Rainfall-induced landslide susceptibility assessment at the Chongren area (China) using frequency ratio, certainty factor, and index of entropy. Geocarto Int 32:139–154. https://doi.org/10.1080/10106049.2015.1130086

Horton RE (1932) Drainage basin characteristics. Eos Trans AGU 13: 350–336. https://doi.org/10.1029/TR013i001p00350

Hou E, Wang J, Chen W (2017) A comparative study on groundwater spring potential analysis based on statistical index, index of entropy and certainty factors models. Geocarto Int 33(7):754–769. https://doi.org/10.1080/10106049.2017.1299801

Ihara S (1993) Information theory for continuous systems. World Scientific Pub Co Inc, Hackensack

Jaafari A, Najafi A, Pourghasemi HR, Rezaeian J, Sattarian A (2014) GIS-based frequency ratio and index of entropy models for landslide susceptibility assessment in the Caspian forest, northern Iran. Int J Environ Sci Technol 11:909–926. https://doi.org/10.1007/s13762-013-0464-0

Jha MK, Chowdary VM, Chowdhury A (2010) Groundwater assessment in Salboni Block, West Bengal (India) using remote sensing, geographical information system and multi-criteria decision analysis techniques. Hydrogeol J 18:1713–1728. https://doi.org/10.1007/s10040-010-0631-z

Kanagaraj G, Suganthi S, Elango L, Magesh N (2019) Assessment of groundwater potential zones in Vellore district, Tamil Nadu, India using geospatial techniques. Earth Sci Inf 12:211–223. https://doi.org/10.1007/s12145-018-0363-5

Khoshtinat S, Aminnejad B, Hassanzadeh Y, Ahmadi H (2019) Groundwater potential assessment of the Sero plain using bivariate models of the frequency ratio, Shannon entropy and evidential belief function. J Earth Syst Sci 128(6). https://doi.org/10.1007/s12040-019-1155-0

Khosravi K, Sartaj M, Tsai FT-C, Singh VP, Kazakis N, Melesse AM, Prakash I, Bui DT, Pham BT (2018) A comparison study of DRASTIC methods with various objective methods for groundwater vulnerability assessment. Sci Total Environ 642:1032–1049. https://doi.org/10.1016/j.scitotenv.2018.06.130

Kumar D, Rao VA, Sarma VS (2014) Hydrogeological and geophysical study for deeper groundwater resource in quartzitic hard rock ridge region from 2D resistivity data. J Earth Syst Sci 123(3):531–543. https://doi.org/10.1007/s12040-014-0408-1

Kumar V, Mondal N, Ahmed S (2020) Identification of groundwater potential zones using RS, GIS and AHP techniques: a case study in a part of Deccan Volcanic Province (DVP), Maharashtra, India. J Indian Soc Remote Sens 48:497–511. https://doi.org/10.1007/s12524-019-01086-3

Lee MJ, Lee JH (2011) Coupled model development between groundwater recharge quantity and climate change using GIS. J Korean Assoc Geogr Inf Stud 14:3651–3651. https://doi.org/10.11108/kagis.2011.14.3.036

Lee S, Lee CW (2015) Application of decision-tree model to groundwater productivity-potential mapping. Sustainability 7:13416–13432. https://doi.org/10.3390/su71013416

Magaia LA, Goto TN, Masoud AA, Koike K (2018) Identifying groundwater potential in crystalline basement rocks using remote sensing and electromagnetic sounding techniques in Central Western Mozambique. Nat Resour Res 27:275–298. https://doi.org/10.1007/s11053-017-9360-5

Magesh N, Chandrasekar N, Soundranayagam J (2012) Delineation of groundwater potential zones in Theni district, Tamil Nadu, using remote sensing, GIS and MIF techniques. Geosci Front 3:189–196. https://doi.org/10.1016/j.gsf.2011.10.007

Moghaddam DD, Rezaei M, Pourghasemi HR, Pourtaghie ZS, Pradhan B (2015) Groundwater spring potential mapping using bivariate statistical model and GIS in the Taleghan Watershed, Iran. Arab J Geosci 8(2):913–929. https://doi.org/10.1007/s12517-013-1161-5

Mokadem N, Boughariou E, Mudarra M, Brahim FB, Andreo B, Hamed Y, Bouri S (2018) Mapping potential zones for groundwater recharge and its evaluation in arid environments using a GIS approach: case study of North Gafsa Basin (Central Tunisia). J Afr Earth Sci 141:107–117. https://doi.org/10.1016/j.jafrearsci.2018.02.007

Mousavi SM, Golkarian A, Naghibi SA, Kalantar B, Pradhan B (2017) GIS-based groundwater spring potential mapping using data mining boosted regression tree and probabilistic frequency ratio models in Iran. AIMS Geosci 3:91–115. https://doi.org/10.3934/geosci.2017.1.91

Naghibi SA, Pourghasemi HR, Pourtaghie ZS, Rezaei A (2014) Groundwater qanat potential mapping using frequency ratio and Shannon's entropy models in the Moghan Watershed, Iran. Earth Sci Inf 8:171–186. https://doi.org/10.1007/s12145-014-0145-7

Naghibi SA, Pourghasemi HR, Dixon B (2016) Groundwater spring potential using boosted regression tree, classification and regression tree, and random forest machine learning models in Iran. Environ Monit Assess 188:44. https://doi.org/10.1007/s10661-015-5049-6

Nampak H, Pradhan B, Manap MA (2014) Application of GIS based data driven evidential belief function model to predict groundwater potential zonation. J Hydrol 513:283–300. https://doi.org/10.1016/j.jhydrol.2014.02.053

Nayak P, Rai AK, Tripathy S (2017) Evaluating groundwater prospects using GIS techniques. Sustain. Water Resour Manag 3:129–139. https://doi.org/10.1007/s40899-017-0082-y

Nhu V-H, Rahmati O, Falah F, Shojaei S, Al-Ansari N, Shahabi H, Shirzadi A, Górski K, Nguyen H, Ahmad BB (2020) Mapping of groundwater spring potential in karst aquifer system using novel ensemble bivariate and multivariate models. Water 12(4):985. https://doi.org/10.3390/w12040985

Oh HJ, Kim YS, Choi JK, Park E, Lee S (2011) GIS mapping of regional probabilistic groundwater potential in the area of Pohang City, Korea. J Hydrol 399:158–172. https://doi.org/10.1016/j.jhydrol.2010.12.027

Ozdemir A (2011) GIS-based groundwater spring potential mapping in the Sultan Mountains (Konya, Turkey) using frequency ratio, weights of evidence and logistic regression methods and their comparison. J Hydrol 411:290–308. https://doi.org/10.1016/j.jhydrol.2011.10.010

Patra S, Mishra P, Mahapatra SC (2018) Delineation of groundwater potential zone for sustainable development: a case study from Ganga Alluvial Plain covering Hooghly district of India using remote sensing, geographic information system and analytic hierarchy process. J Clean Prod 172:2485–2502. https://doi.org/10.1016/j.jclepro.2017.11.161

Paul RS, Rawat U, Sen Gupta D, Biswas A, Tripathi S, Ghosh P (2020) Assessment of groundwater potential zones using multi-criteria evaluation technique of Paisuni River Basin from the combined state of Uttar Pradesh and Madhya Pradesh, India. Environ Earth Sci 79(13). https://doi.org/10.1007/s12665-020-09091-3

Pourghasemi HR, Pradhan B, Gokceoglu C (2012) Application of fuzzy logic and analytical hierarchy process (AHP) to landslide susceptibility mapping at Haraz watershed, Iran. Nat Hazards 63(2):965–996. https://doi.org/10.1007/s11069-012-0217-2

Pradhan B (2009) Groundwater potential zonation for basaltic watersheds using satellite remote sensing data and GIS techniques. Open Geosci 1:120–129. https://doi.org/10.2478/v10085-009-0008-5

Rahmati O, Samani AN, Mahdavi M, Pourghasemi HR, Zeinivand H (2015) Groundwater potential mapping at Kurdistan region of Iran using analytic hierarchy process and GIS. Arab J Geosci 8:7059–7071. https://doi.org/10.1007/s12517-014-1668-4

Rahmati O, Pourghasemi HR, Melesse AM (2016) Application of GIS-based data driven random forest and maximum entropy models for groundwater potential mapping: a case study at Mehran region, Iran. Catena 137:360–372. https://doi.org/10.1016/j.catena.2015.10.010

Rajaveni S, Brindha K, Elango L (2015) Geological and geomorphological controls on groundwater occurrence in a hard rock region. Appl Water Sci 7:1377–1389. https://doi.org/10.1007/s13201-015-0327-6

Rana R, Ganguly R, Gupta AK (2018) Indexing method for assessment of pollution potential of leachate from non-engineered landfill sites and its effect on ground water quality. Environ Monit Assess 190:46. https://doi.org/10.1007/s10661-017-6417-1

Rao YS, Reddy T, Nayudu P (2000) Groundwater targeting in hard rock terrain using fracture pattern modelling, Niva river basin, Andhra Pradesh, India. Hydrogeol J 8:494–502. https://doi.org/10.1007/s100400000090

Rashid M, Ahmad Lone M, Ahmed S (2011) Integrating geospatial and ground geophysical information as guidelines for groundwater potential zones in hard rock terrains of south India. Environ Monit Assess 184(8):4829–4839. https://doi.org/10.1007/s10661-011-2305-2

Reddy GPO, Babu RS, Rao MS (1994) Hydro-geology and hydro-geomorphological conditions of Anantapur district (AP), India. Indian Geograph J 69(2):128–135

Reddy GPO, Maji AK, Srinivas CV, Kamble KH, Velayutham M (2002) GIS-based basin morphometric information system for terrain and resources analysis. In: Patil VC et al (eds) Agro-informatics, pp 37–42

Reddy GPO, Kumar N, Sahu N, Singh SK (2018) Evaluation of automatic drainage extraction thresholds using ASTER GDEM and Cartosat-1 DEM: a case study from basaltic terrain of Central India. Egypt J Remote Sens Space Sci 21(1):95–104. https://doi.org/10.1016/j.ejrs.2017.04.001

Ren X, Li P, He X, Su F, Elumalai V (2021) Hydrogeochemical processes affecting groundwater chemistry in the central part of the

Guanzhong Basin, China. Arch Environ Contam Toxicol 80(1):74–91. https://doi.org/10.1007/s00244-020-00772-5

Rodell M, Velicogna I, Famiglietti JS (2009) Satellite-based estimates of groundwater depletion in India. Nature 460(7258):999–1002. https://doi.org/10.1038/nature08238

Saha D, Dwivedi SN, Roy GK, Reddy DV (2013) Isotope-based investigation on the groundwater flow and recharge mechanism in a hard-rock aquifer system: the case of Ranchi urban area, India. Hydrogeol J 21:1101–1115. https://doi.org/10.1007/s10040-013-0974-3

Sahoo S, Munusamy SB, Dhar A, Kar A, Ram P (2017) Appraising the accuracy of multi-class frequency ratio and weights of evidence method for delineation of regional groundwater potential zones in canal command system. Water Resour Manag 31:4399–4413. https://doi.org/10.1007/s11269-017-1754-y

Saranya T, Saravanan S (2020) Groundwater potential zone mapping using analytical hierarchy process (AHP) and GIS for Kancheepuram District, Tamilnadu, India. Model Earth Syst Environ 6:1105–1122. https://doi.org/10.1007/s40808-020-00744-7

Sashikkumar M, Selvam S, Kalyanasundaram V, Johnny J (2017) GIS based groundwater modeling study to assess the effect of artificial recharge: a case study from Kodaganar river basin, Dindigul district, Tamil Nadu. J Geol Soc India 89:57–64. https://doi.org/10.1007/s12594-017-0558-2

Selvam S, Magesh N, Chidambaram S, Rajamanickam M, Sashikkumar M (2015) A GIS based identification of groundwater recharge potential zones using RS and IF technique: a case study in Ottapidaram taluk, Tuticorin district, Tamil Nadu. Environ Earth Sci 73:3785–3799. https://doi.org/10.1007/s12665-014-3664-0

Selvarani AG, Elangovan K, Kumar C (2016) Evaluation of groundwater potential zones using electrical resistivity and GIS in Noyyal River basin, Tamil Nadu. J Geol Soc India 87:573–582. https://doi.org/10.1007/s12594-016-0431-8

Şener E, Şener Ş, Davraz A (2018) Groundwater potential mapping by combining fuzzy-analytic hierarchy process and GIS in Beyşehir Lake Basin, Turkey. Arab J Geosci 11:1–21. https://doi.org/10.1007/s12517-018-3510-x

Shaban A, Khawlie M, Abdallah C (2006) Use of remote sensing and GIS to determine recharge potential zone: the case of occidental Lebanon. Hydrogeol J 14:433–443. https://doi.org/10.1007/s10040-005-0437-6

Sharma A, Ganguly R, Gupta AK (2020) Impact assessment of leachate pollution potential on groundwater: an indexing method. J Environ Eng 146(3):05019007. https://doi.org/10.1061/(ASCE)EE.1943-7870.0001647

Shi H, Tiejian L, Wei J, Fua W, Wang G (2016) Spatial and temporal characteristics of precipitation over the three-river headwaters region during 1961-2014. J Hydrol Reg Stud 6:52–65. https://doi.org/10.1016/j.ejrh.2016.03.001

Shivanna K, Kulkarni UP, Joseph TB, Navada SV (2004) Contribution of storms to groundwater recharge in the semi-arid region of Karnataka. India. Hydrol Process 18:473–485. https://doi.org/10.1002/hyp.1323

Siahkamari S, Haghizadeh A, Zeinivand H, Tahmasebipour N, Rahmati O (2018) Spatial prediction of flood-susceptible areas using frequency ratio and maximum entropy models. Geocarto Int 33:927–941. https://doi.org/10.1080/10106049.2017.1316780

Singh SK, Chatterji S, Chattaraj S, Butte PS (2016) Land Resource Inventory (LRI) on 1:10000 scale, Why and How? NBSS Publ. No. 172. ICAR- National Bureau of Soil Survey and Land Use Planning, Nagpur, India. 94p

Singha SS, Pasupuleti S, Singha S, Singh R, Venkatesh AS (2019) Analytic network process based approach for delineation of groundwater potential zones in Korba district, Central India using remote sensing and GIS. Geocarto Int:1–22. https://doi.org/10.1080/10106049.2019.1648566

Song S-H, Choi K-J (2012) An appropriate utilization of agricultural water resources of Jeju island with climate change (I). J Soil Groundw Environ 17:62–70. https://doi.org/10.7857/JSGE.2012.17.2.062

Su Z, Wu J, He X, Elumalai V (2020) Temporal changes of groundwater quality within the groundwater depression cone and prediction of confined groundwater salinity using Grey Markov model in Yinchuan area of northwest China. Expo Health 12(3):447–468. https://doi.org/10.1007/s12403-020-00355-8

Suganthi S, Elango L, Subramanian SK (2013) Groundwater potential zonation by Remote Sensing and GIS techniques and its relation to the Groundwater level in the Coastal part of the Arani and Koratalai River Basin, Southern India. Earth Sci Res J 17:87–95

Taylor RG, Scanlon B, Döll P, Rodell M, van Beek R, Wada Y, Longuevergne L, Leblanc M, Famiglietti JS, Edmunds M, Konikow L, Green TR, Chen J, Taniguchi M, Bierkens MFP, MacDonald A, Fan Y, Maxwell RM, Yechieli Y, Gurdak JJ, Allen DM, Shamsudduha M, Hiscock K, Yeh PJF, Holman I, Treidel H (2013) Groundwater and climate change. Nat Clim Chang 3(4):322–329. https://doi.org/10.1038/nclimate1744

Tehrany MS, Shabani F, Jebur MN, Hong H, Chen W, Xie X (2017) GIS-based spatial prediction of flood prone areas using standalone frequency ratio, logistic regression, weight of evidence and their ensemble techniques. Geomat Nat Hazards Risk 8(2):1538–1561. https://doi.org/10.1080/1947570017.13620385.2

Tolche A (2020) Groundwater potential mapping using geospatial techniques: a case study of Dhungeta-Ramis sub-basin, Ethiopia. Geol Ecol Landsc 5(1):65–80. https://doi.org/10.1080/24749508.2020.1728882

Wang D, Wu J, Wang Y, Ji Y (2020) Finding high-quality groundwater resources to reduce the hydatidosis incidence in the Shiqu County of Sichuan Province, China: analysis, assessment, and management. Expo Health 12(2):307–322. https://doi.org/10.1007/s12403-019-00314-y

Wei P, Lu Z, Song J (2015) Variable importance analysis: a comprehensive review. Reliab Eng Syst Saf 142:399–432. https://doi.org/10.1016/j.ress.2015.05.018

Woo NC (2013) Climate change and groundwater sustainability in Korea for next decade. J Soil Groundw Environ 18:1–5. https://doi.org/10.7857/JSGE.2013.18.1.001

Yufeng S, Fengxiang J (2009) Landslide stability analysis based on generalized information entropy. Int Conf Environ Sci Inf Appl Technol 2:83–85. https://doi.org/10.1109/ESIAT.2009.258